FEBS Letters 587 (2013) 1863–1869

FEBS Letters

journal homepage: www.FEBSLetters.org

Review

Inorganic pyrophosphatases: One substrate, three mechanisms

Kajander Tommi [a,*], Kellosalo Juho [b], Goldman Adrian [a,b,*]

[a] Institute of Biotechnology, University of Helsinki, Helsinki, Finland
[b] Department of Biosciences, Division of Biochemistry, University of Helsinki, Helsinki, Finland

ARTICLE INFO

Article history:
Received 3 May 2013
Accepted 6 May 2013
Available online 16 May 2013

Edited by Alexander Gabibov, Vladimir Skulachev, Felix Wieland and Wilhelm Just

Keywords:
Pyrophosphatase
Structure
Membrane protein
Ion pump
Catalysis
Phosphorolysis

ABSTRACT

Soluble inorganic pyrophosphatases (PPases) catalyse an essential reaction, the hydrolysis of pyrophosphate to inorganic phosphate. In addition, an evolutionarily ancient family of membrane-integral pyrophosphatases couple this hydrolysis to Na^+ and/or H^+ pumping, and so recycle some of the free energy from the pyrophosphate. The structures of the H^+-pumping mung bean PPase and the Na^+-pumping *Thermotoga maritima* PPase solved last year revealed an entirely novel membrane protein containing 16 transmembrane helices. The hydrolytic centre, well above the membrane, is linked by a charged "coupling funnel" to the ionic gate about 20 Å away. By comparing the active sites, fluoride inhibition data and the various models for ion transport, we conclude that membrane-integral PPases probably use binding of pyrophosphate to drive pumping.

1. Introduction

Inorganic pyrophosphatases (PPases) are essential enzymes that are important in controlling the cellular concentration of inorganic pyrophosphate (PP_i) and thus driving biosynthetic reactions like nucleic acid and protein synthesis to completion. PP_i is formed in large quantities as a by-product of biosynthetic reactions [1], and the PP_i concentration affects the intracellular equilibria of these important physiological reactions. PPases catalyse the simplest phosphoryl transfer reaction imaginable, the hydrolysis of the symmetrical pyrophosphate (PP_i) substrate to two molecules of inorganic phosphate (P_i).

Of the four different classes of PPases (membrane-integral M-PPase and the soluble Family I, Family II and Family III PPases), the Family III S-PPases [2], which are in fact modified haloalkane dehalogenases, have not been extensively characterised and are present in only a few bacterial species. We therefore focus on the other three PPase families, as they represent enzyme solutions that are mostly or entirely devoted to pyrophosphatase catalysis. The first crystals of a pyrophosphatase were reported over 50 years ago [3]. What have we learnt about the structures and mechanisms in this time?

1.1. Commonalities and differences

Catalysis by PPases requires three or four metal ions [4–7], depending on the enzyme family, pH and PP_i concentration. The catalysis is based on leaving group activation and effective nucleophile generation and proceeds without an enzyme–phosphate intermediate [8–12]. This suggests that in each case catalysis happens inside an inorganic metal–phosphate cage, with the protein side-chains occupying mostly supporting roles [9,13]. Three of the biggest differences between the various enzymes in terms of pyrophosphate hydrolysis are their responses to two different inhibitors: fluoride, and the diphosphonates, especially to aminomethylenediphosphonate (AMDP), as well as the types of divalent cations required (Table 1). In terms of catalysis M-PPases are the slowest ($k_{cat} \approx 10\ s^{-1}$), while the activity of family I PPases is roughly one order of magnitude higher ($k_{cat} \approx 200\ s^{-1}$) and that of family II enzymes again one order of magnitude higher than the activity of family I enzymes ($k_{cat} \approx 2000\ s^{-1}$) (Table 1).

Due to the detailed structural and functional information available, the soluble PPases, especially the Family I enzymes, represent one of the better understood phosphoryl-transfer enzymes. Precise mechanisms have been proposed to account for their catalytic efficiency, a factor of 10^{10-11} compared with the rate of PP_i hydrolysis in solution [4,14]. The biological function of the Family I and

* Corresponding authors. Addresses: Institute of Biotechnology, P.O. Box 65, University of Helsinki, 00014 Helsinki, Finland (T. Kajander), Department of Biosciences, Division of Biochemistry, P.O. Box 56, University of Helsinki, 00014 Helsinki, Finland (A. Goldman).

E-mail addresses: tommi.kajander@helsinki.fi (T. Kajander), adrian.goldman@helsinki.fi (A. Goldman).

0014-5793/$36.00
http://dx.doi.org/10.1016/j.febslet.2013.05.003

Table 1
Selected kinetic properties of PPases and their inhibition by F^- and AMDP.

	Mg^{2+}	Mn^{2+}	K_i for AMDP (μM)	K_i for F^- (μM)*	k_{cat} (s^{-1})
Family I PPase	Req.		11–150 [62–64]	⩽11–90 [65,66]	200–400 [67]
Family II PPase	Req.	Activates	1000 [64]	6* [68]	1700–3000 [33]
M-PPase	Req.		1.2–1.8 [63,69]	3000–4800 [63]	3.5–20 [70,71]

* In the presence of Mg^{2+}. The K_i for F^- inhibition in Family II PPases in the presence of Mn^{2+} is much higher, because Mn^{2+} binds F^- poorly. Req. = required for function.

Family II PPases is also identical, as their sole purpose is the removal of pyrophosphate, although only the Family II PPases include members that are allosterically regulated [15]. As we discuss below, Family I and Family II PPase sequences and structures are unrelated, and the mechanisms, too, seem not to be the same. Membrane integral PPases (M-PPases), on the other hand, are very different to their soluble counterparts; they are functionally (but not structurally) similar to membrane integral ATPases in that they couple P–O–P anhydride hydrolysis/synthesis to the pumping of protons or sodium ions. M-PPases have also a broader biological function than soluble PPases as they are crucial for the survival of plants and bacteria under various low-energy stress conditions (see below) [16–18].

In the discussion that follows we endeavour to combine our current knowledge of the structures and mechanisms of PPases including their differential sensitivity to inhibition by F^- (Table 1) to try to distinguish between three different proposals for coupling pyrophosphate hydrolysis to ion pumping in M-PPases [12,19,20].

2. Structure and mechanism of soluble pyrophosphatases

Family I PPases, first crystallised in 1952 [3], have been extensively-studied, especially those from *Escherichia coli* (EPPase) [13,21] and *Saccharomyces cerevisiae* (YPPase) [9,14,22–25] well characterised. The work has included atomic resolution structures [25] as well as extensive structures of mutants that have led to a full structural description of the entire catalytic cycle [14]. Family I PPases are found in all kingdoms of life.

Family I PPases fold into a compact single domain structure, the core of which is a conserved five-strand OB-fold β-barrel [9] on top of which sits the active site (Fig. 1). The oligomeric states vary, as the eukaryotic enzymes are usually dimers [26], while the bacterial enzymes are typically hexamers [27]. The eukaryotic enzymes are larger; YPPase has an extra β-sheet and N- and C-terminal extensions to the core structure. Even though sequence conservation in Family I PPases barely extends outside the 20 charged and hydrophilic residues in the active site, they can be reliably identified by the conserved D-(S/G/N)-D-P-*ali*-D-*ali*-*ali* motif (*ali* = C/I/L/M/V) [28]. This motif contains D120, which binds the two activating metal ions M1 and M2 present before substrate binds (Fig. 2), as well as D117, which helps activate the water molecule [25]. The distinguishing features of catalysis in family I PPases are that all lone pairs in the substrate are coordinated and that PPi hydrolysis is carried out by an associative mechanism in which an activated water molecule nucleophile attacks the electrophilic phosphate moiety of PP_i. The water, activated by M1, M2 and D117, deprotonates at pH 6 [13]. The metal-coordination of the nucleophile makes the family I PPases very susceptible to F^- inhibition as this ion can easily replace the incipient hydroxide ion, and an inhibited complex ($E:Mg_4FPP_i$) is stable enough to be isolated chromatographically [29]. In the substrate-bound state of Family I PPases, the binding of the electrophilic phosphate of PP_i is coordinated by metal ions, while the leaving group phosphate is bound by the protein side-chains (Fig. 2). This is consistent with the idea that activating the leaving group by partial transfer of a proton is more effective than activation by a metal ion [9].

Family II PPases, identified only 15 years ago [30,31], occur in bacterial and archael lineages, in particular *Bacilli* and *Clostridia*, including several human pathogens. Family II PPases are structurally completely unrelated to Family I PPases [10,11] (Fig. 1); these homodimeric two domain proteins belong to the "DHH" phosphoesterase superfamily [32], where DHH refers to a conserved Asp-His-His motif in the N-terminal domain that is critical for metal ion binding specificity. Other proteins in this family include cytosolic exopolyphosphatases, a cyclic AMPase and RecJ, a single-stranded DNA exonuclease [32]. The active site of Family II PPases is located between the N-terminal DHH and C-terminal DHHA2 domains [10,11]. About a quarter of them also contain additional

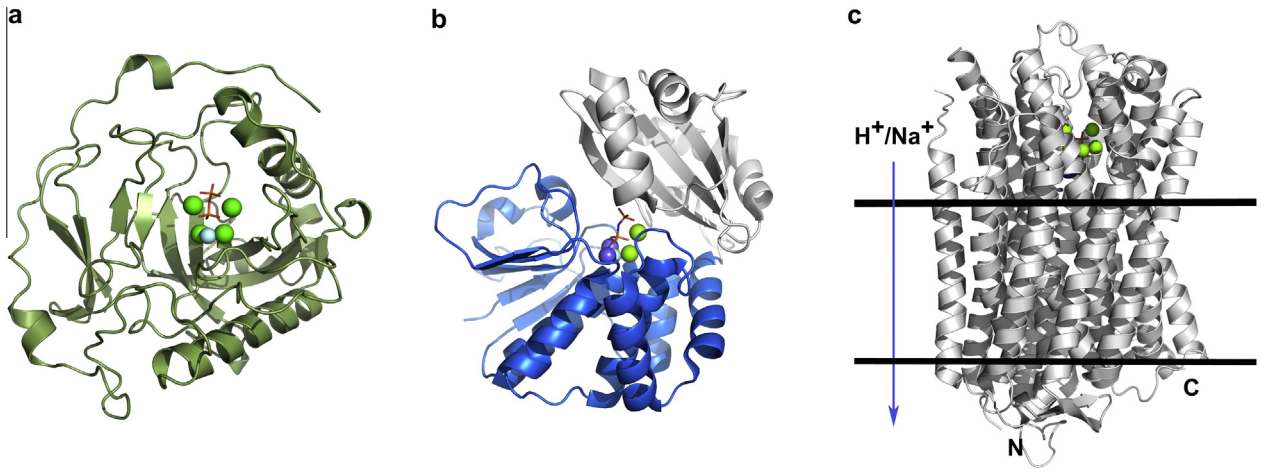

Fig. 1. Side by side comparison of overall ribbon views of substrate bound conformations of Family I yeast PPase (YPPase, left) (1E6A [25]), Family II *B. subtilis* PPase (BsPPase. middle) (2HAW [4]) and H^+-pumping mung bean PPase (VrPPase, right) (4A01 [12]). The domain structure is shown, as is the membrane region in mung bean PPase. This and Fig. 2 were drawn with PyMol (The PyMOL Molecular Graphics System, Version 1.2r3pre, Schrödinger, LLC).

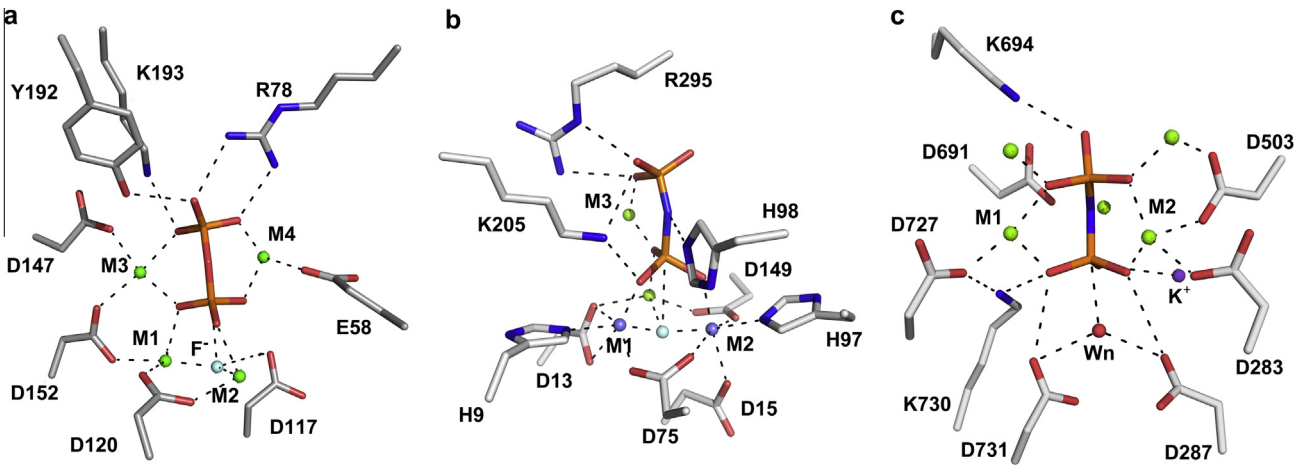

Fig. 2. Side by side comparison of the hydrolytic sites of YPPase (left), BsPPase (middle) and VrPPase (right), emphasising the difference in detailed active site geometry between the three enzymes. In all cases the scissile bond is vertical, with the nucleophile directly underneath. Key side chains are shown in atom colours, as are Mg^{2+} (green), F^- (cyan), the Mn^{2+} (BsPPase) light purple, and the K^+ (VrPPase) purple. The nucleophilic water in VrPPase is labelled Wn and shown in red; the electrophilic phosphorus P1 is the lower in each figure. Hydrogen bonds and ionic interactions are shown as dotted lines.

regulatory domains such as CBS and DRTGG domains inserted in the first DHH domain [15].

As stated above, Family II PPases show highest catalytic activity in the presence of transition metal ions Mn^{2+} or Co^{2+}, which bind to the enzyme with nanomolar affinity, while they show lower activity with Mg^{2+}, which binds with just micromolar affinity [33]. The binding and kinetic preference for transition metals can be understood on the basis of the architecture of the active site. First, even though M1 and M2 are coordinated by a single Asp as in Family I PPases [11], they are also coordinated by H9 and H97 (Fig. 2) in Family II PPases. This leads to the strong preference for Mn^{2+} in the active site, as transition metals prefer soft ligands such as Cys or His, while Mg^{2+} prefers carboxylates. Second, catalysis is faster in the presence of Mn^{2+} because of changes in metal coordination. During catalysis, the C-terminal domain closes over the N-terminal domain, and the coordination of M2 changes from five-coordinated to six-coordinated [4,34]. Transition metals tolerate this change much better than Mg^{2+}.

The structure of the substrate bound-state of *Bacillus subtilis* PPase (BsPPase) [4] shows coordination of a nucleophile in the active site by three metal ions: M1, M2 and M4 (Fig. 2). This tri-metal coordination could explain why Family II enzymes with Mg^{2+} bound have a higher affinity for F^- than Family I enzymes (Table 1), while the tri-metal coordination and stronger F^- binding together suggest that Family II PPases deprotonate the water molecule even more effectively than Family I PPases. Finally, the substrate-bound structures show that H98 is positioned to donate a proton to the leaving group phosphate (Fig. 2). This, and the distortion of the substrate molecule seen in our high-resolution structures, led us to suggest that, unlike Family I PPases, Family II PPases could employ a dissociative mechanism [4], where a strong electrophile, such as metaphosphate, could "pull" the hydroxide in for nucleophilic attack. Overall, Family I and Family II PPases are thus not related in sequence, structure nor apparent catalytic mechanism, even though the formal reaction is the same. We return to this point below.

3. Membrane-integral pyrophosphatases

M-PPases have a completely different architecture and function, as they are primary ion pumps in plants, algae and some protozoans, bacteria and archae, producing proton and/or sodium gradients. They are reversible, coupling the phoshorolysis/synthesis of PP_i to H^+ and/or Na^+ pumping [35]. They are highly hydrophobic ion pumps with no recognisable separate soluble domains. The structure of these enzymes was unknown until just last year, when the structures of the mung bean PPase (VrPPase) and *T. maritima* PPase (TmPPase) were solved [12,19]. Before then, only the positions of conserved sequence motifs involved in metal binding and PP_i hydrolysis, and the topology and organisation of the secondary structure of the enzyme were known [16]. Mutational analysis and sequence comparison identified three conserved cytoplasmic "acidic motifs" necessary for activity between TM helices 5 and 6, 11 and 12, and 15 and 16. FRET-measurements [36], and studies with covalent inhibitors [37–42] showed that ligand binding causes the movement of the conserved motifs and the protection of various conserved residues (TmPPase: R191, K199, D232, K499, C599 and H681).

M-PPases are an evolutionarily ancient protein family. In eukaryotes, they occur predominantly in the vacuolar membranes of plants [43] and in the acidocalcisomal (acidic calcium storage compartments) membranes of protista [44]. They occur in species where energy limitation is frequent, and are important under starvation and stress conditions (drought, nutrient deficiency, anoxia, cold stress, low-light intensity, salt stress) to provide ion gradients when ATP is scarce [16–18]. In plants, however, M-PPase is also necessary for the removal of PP_i during maturation [45]. Elegant detective work by the Lahti and Baykov laboratories has shown that M-PPases can be divided into four families (see below) based on their ion-pumping specificity, Na^+ and/or H^+, and whether they are activated by K^+ or not [35,46,47]. Unsurprisingly, Na^+-pumping M-PPases have an absolute requirement for Na^+ (or Li^+) for enzymatic activity [47,48].

3.1. Structure

Membrane PPases have a single large transmembrane domain with 15–17 transmembrane (TM) helices [49] with large hydrophilic regions on the cytoplasmic side of the protein. All M-PPases studied so far are homodimeric, although the active site is contained within a single monomer [19].

The structures of VrPPase with imidodiphosphate (PNP) bound [12] and of TmPPase with product bound [19] are, as expected, very similar (root mean square deviation/Cα 1.57 Å), suggesting that the hydrolytic mechanism is conserved, while the ion

specificity varies. Both structures reveal a dimer of two 80 kDa monomers with 16 transmembrane helices, with an unusual internal organisation of three intertwined four-helix "splayed bundles" formed from TM 3–6, 9–12 and 13–16. These form the core of the monomer structure. The TM-helices extend above the lipid bilayer on the cytoplasmic side by about 20 Å (Fig. 1), and the catalytic residues thought to reside in the cytoplasmic loops actually occur on these long helices (Fig. 1). The structure is a unique new membrane protein structure, completely unrelated to *e.g.* the ATPase ion pumps or – more obviously – the soluble PPases.

The functional core of the ion pump is formed by six central helices, TM 5–6, 11–12, and 15–16. There are four catalytic regions: the hydrolytic centre, where the inhibitor PNP and product bind in the solved structures, a unique "coupling funnel" [19], an ion gate formed by charged residues and the exit channel towards the luminal or periplasmic side of the membrane. In all solved structures the gate and exit channel are closed. The hydrolytic centre is well above the membrane plane and the coupling funnel cuts through the membrane with the gate in approximately in the middle of the membrane. The distance from the gate to the PP_i binding site is about 20 Å. The active site is closed by a long loop between TM 5 and 6 (residues 206–225 in TmPPase) on substrate binding, and opened again after the hydrolysis and pumping have occurred (see below) [12,19]. This loop movement explains the results of FRET measurements and the protection of conserved residues from modification upon ligand binding [36–42] (see above).

In the VrPPase hydrolytic centre, the inhibitor PNP is coordinated by five Mg^{2+}-ions and conserved lysines 250, 694 and 730 (TmPPase K199, K663 and K695), residing in TMs 5, 15 and 16, respectively. The Mg^{2+}-ions are coordinated by six conserved Asps 253, 257, 283, 507, 691 and 727 in the six central helices. Residues of the "acidic motif" (see above) in the loop between TM 5 and 6 do not take part directly in substrate binding, even though earlier trypsin digestion [50] and enzyme activity measurements [51,52] seemed to indicate so. However, they form an intricate salt-bridge network together with conserved lysines, arginines and aspartates found in TM 5, 12, 13 and 15 that seems to play a major part in the closing of the active site cavity upon substrate binding.

Of the five Mg^{2+} seen in the hydrolytic centre, two are part of the Mg_2PPi substrate [5], and two are the previously identified [5,6] activating Mg^{2+}-ions. The fifth Mg^{2+}-ion is putatively inhibiting, which, even though it has very low binding affinity ($K_d \approx 100$ mM, [53]), could well bind due to the high $MgCl_2$-concentration (0.2 M) in which the protein was crystallised. In addition to the Mg^{2+}-ions, there is also a K^+ ion, which coordinates the electrophilic phosphorus (P1) of the PNP (Fig. 2). The hydrolytic centre also contains a water molecule coordinated by the conserved aspartates D287 and D731 (D236 and D696 in TmPPase) that is positioned for inline nucleophilic attack on the P1 (see Section 3.3).

The hydrolytic centre is connected to the ionic gate (below) by an unusual "coupling funnel" [12,19] consisting of an ionic network of eight conserved residues, the mutation of which has major effects on function [43]. In particular there appears to be a switch connected to conformational changes around R191 and K499 (TmPPase) and D236; R191 forms long range ionic interactions with D236 and D243 in the unbound state and binds to the backbone carbonyl of G237, acting as a switch between the two sites, the conformation depending on whether the substrate is bound or not.

D243, linked to the coupling funnel *via* R191, is part of the ion gate triplet of D243-K707-D246. The gate is closed in all structures solved so far. All Na^+ M-PPases, H^+/Na^+ M-PPases and K^+-independent H^+ M-PPases and the *Carboxydothermus hydrogenformans* type K^+-dependent H^+ M-PPases have an ion triplet, while in the other K^+-dependent H^+ M-PPases the ion triplet is replaced by an ion pair equivalent to D243-K707 [54]. In plant K^+-dependent H^+ M-PPases, there is a glutamate at the position equivalent to 250 (*i.e.* one turn further down TM6 than in TmPPase), while in *Flavobacterium johnsoniae* type M-PPases, the Glu residue is at the equivalent height but on TM5 (TmPPase 184) [54]. Mutational studies show that the E246S and G250E changes abolish Na^+-pumping but without leading to proton pumping, while the E185S (TmPPase 184) and E235S (TmPPase 250) changes in *F. johnsoniae* and *Leptospira biflexa* M-PPase, respectively, uncouple H^+ pumping [54]. It is clear that changes around the gate are essential for ion selectivity, but how remains unclear. Below the gate is the hydrophobic exit channel [12,19] that is closed in all the structures seen and so prevents ion translocation. There are neither charged residues nor significant sequence conservation in the exit channel.

3.2. Evolution of membrane PPases

M-PPases are abundant in sequence data banks – and found in all kingdoms of life except the multicellular animals and fungi. All the plant species studied have M-PPases [43] while, in algae, only glaucophytes lack them. They are not as universal in protozoans and prokaryotes. In prokaryotes, the distribution can also be variable within a group, *e.g.* amongst *Clostridium* bacteria, some have M-PPases while others do not, which may be related to their respective environmental niches. Phylogenetic and functional analyses have so far revealed four families of M-PPases. There are K^+-independent M-PPases, which all pump protons, and three varieties of K^+-dependent M-PPases: H^+-pumps, Na^+-pumps, and Na^+ and H^+-pumps [35]. Why is this so?

The utilisation of PP_i to provide chemical energy may well have occurred early in evolution before the adoption of ATP as an energy source [55]. M-PPases might therefore have been the very first enzymes coupling hydrolysis or formation of the phosphoanhydride bond to changes in electrical potential across membranes [56]. As membranes are less leaky to sodium ions than protons, the use of Na^+ could have preceded the use of H^+ in the creation of membrane potential [57,58]. The first M-PPases should therefore have been Na^+-PPases, and indeed sequence analysis suggests that this is true: Na^+-PPases, which represent the majority of the K^+ dependent M-PPases, form a monophyletic clade, while the H^+-PPases form several independent clades [54], suggesting that they evolved independently from the Na^+-PPases at least four times [20]. In addition, Baykov and co-workers [20] point out that the enzymes in each clade of K^+-dependent H^+-M-PPases come from highly-related organisms and have very similar sequences, indicating recent evolutionary events. For instance, in the Na^+/H^+ M-PPases, four residues constitute a sequence signature: T/S82, F86, D140 and M176 (TmPPase numbering) [35], and M-PPases from the same clade that lack one or more of the residues do not show dual pumping [35]. The evolution of Na^+/H^+ M-PPases thus presumably occurred separately from the evolution of H^+-specificity [35].

One well-established fact is the basis of K^+-dependence. As Belogurov and Lahti showed [46], A495 (TmPPase numbering) is replaced by K495 in the K^+-independent enzymes, and the single A→K point mutation is sufficient to convert a K^+-dependent enzyme into a K^+-independent one. In both the TmPPase and VrPPase structures, the K^+ ion binds the electrophilic phosphate group in the active site. Modelling the A495K mutation in TmPPase suggested that the Lys residue could coordinate the phosphate and increase its electrophilicity, as the K^+ apparently does. There seems to be interplay between the potassium and sodium binding in Na^+ M-PPases and in H^+/Na^+ M-PPases: potassium binding lowers the K_a of sodium activation [35,47,53,54], but the mechanism is not clear.

Intriguingly, there is internal threefold symmetry in the M-PPase structure: we were able to superimpose the splayed 4-helix

bundles 3–6, 9–12 and 13–16 on each other with an r.m.s.d per Cα of 2.1–2.9 Å [19]. The superposition also aligns key conserved active site residues including twelve active site aspartates: D202^{5}-D465^{11}-D660^{15}, D228^{6}-D488^{12}-D688^{16}, D232^{6}-N442^{12}-D692^{16}, D236^{6}-A496^{12}-D696^{16} and D243^{6}-I503^{12}-D703^{16} (superscripts refer to which helix the residue is on) [19]. This proves that M-PPases have evolved through gene triplication, as previously hypothesised [59]. Internal trimeric symmetry perpendicular to the membrane plane is unusual in membrane proteins, where gene duplication usually gives rise to dyad symmetry perpendicular to the membrane plane.

3.3. Membrane PPase pump mechanism, specificity and catalysis

The now available structures of M-PPases capture the three major states of the catalytic cycle: the resting state (TmPPase) [19], the inhibitor complex (VrPPase) [12] and the product complex (TmPPase) [19]. Comparing these individual states and so following the motions during the catalytic cycle reveals that, in the inhibitor/product-bound states, the hydrolytic centre is closed by ordering of the TM5–6 loop, by contraction of the "coupling funnel", due to the movement of TM11–12 and 15–16 towards the centre of the funnel, and by a piston-like "downward" movement of TM12 of at least 2 Å, concomitant with bending of TM11 at a hinge. Is it possible that a larger transient downward motion of TM11–12 upon substrate binding would open the gate to release the ion to the exit channel [19]?

The two most poorly-understood aspects of the mechanism are coupling of ion pumping to hydrolysis and ion selectivity. Clearly, the Na^+ in the Na^+-pumps needs to bind near the gate, where there are several carboxylate groups available for coordination of the ion. It seems reasonable to suppose that the extra formal negative charge in the E246-K707-D243 ion triple is necessary for this, especially as in certain clades of H^+-PPases, there is no E246, but instead, one turn lower down, E184 or E250 on TM5 or TM6 E250 (see above). This suggests, at least to us, that these are protonated in the resting state and so a Grotthus or even tunnelling mechanism may allow pumping. Certain clades of H^+ M-PPases retain the E246 in the ion triple but are proton pumps [54]. In this case, the E246 might not actually take part in the ion-triple, so that a similar mechanism to the one proposed above for E284/E250 H^+-pumps might occur. As H^+/Na^+ M-PPases can transport both Na^+ and protons without mutual inhibition [35], there may be two gates or at least two binding sites from which the Na^+ and H^+ are released, though the exit channel may be similar. This may be related to the sequence motif on TM-3 and 4 (see above), especially the D140, which is in the membrane and likely to be protonated in the resting state. As Baykov and co-workers suggest [20], allosteric pumping, by which one monomer pumps protons and the other sodium ions, seems highly unlikely as there is no structural evidence so far for an asymmetric complex.

There are currently three proposals for how ion pumping is coupled to hydrolysis/synthesis of the phosphoanhydride bond. We proposed that these motions occur upon binding of substrate and before hydrolysis (see above) [19]: this corresponds to a "binding change" type mechanism. Lin and co-workers [12] suggested that the proton release from the water nucleophile upon PP_i hydrolysis would drive release at the gate *via* a Grotthus type mechanism: this is similar to bacteriorhodopsin, while Baykov and co-workers [20] very recently suggested that a third model. They agree with us that conformational change must be important but, instead of the binding change model we proposed, they suggest Mitchell's "direct-coupling" [60] where the proton generated during hydrolysis is directly transported [20] or directly leads to displacement of the sodium ion. However, as they state, this requires that the catalytic centre and the gate are in close proximity, while there actually is a 20 Å coupling funnel between the sites. Conversely, we also do not support a bacteriorhodopsin-type model [12,61]. Bacteriorhodopsin is an irreversible proton pump, whereas M-PPases are reversible proton pumps. Finally, neither of the competing models suggests a major role for the observed conformational changes, and neither of them convincingly provides a unifying mechanism explaining how small changes convert a Na^+-pump into an H^+-pump. In the Na^+-pumps, the proton released during hydrolysis is released to the cytoplasm, so any mechanism where the proton from hydrolysis directly drives pumping requires a large change in mechanism to generate an H^+-pump from a Na^+-pump. In the next section, we compare and contrast the three hydrolytic mechanisms of Family I-, Family II- and M-PPases for further insight into this conundrum.

4. Hydrolysis in PPases and the implications for pumping

At first glance, Family I and Family II soluble PPases seem to have quite similar solutions to catalysis of the hydrolysis step. Three metal ions, the nucleophilic water/hydroxide ion and the position of the phosphate groups all superimpose in the active sites [11]. The reality is quite different; they use different activating metal ions and they appear to activate the water molecule nucleophile and leaving group differently (see above). Of special interest is the coordination at the nucleophile: in Family I PPases, just two metal ions coordinate the water molecule, while in Family II PPases three metal ions coordinate the nucleophile, which is located *away* from the electrophilic phosphoryl group (Fig. 2). Also, the substrate is distorted, possibly even forming a metaphosphate (Fabrichniy & Goldman, unpublished), which would increase the electrophilicity of the phosphorous [4]. These changes are consistent with the fact that Family II PPases have higher k_{cat} and bind fluoride ion about twofold tighter than Family I PPases (Table 1); there is more positive charge in the active site. What does this tell us about the M-PPases?

In contrast to the soluble PPases, M-PPases are very poor catalysts, with turnover numbers about two orders of magnitude slower under optimal conditions (Table 1). M-PPases seem to achieve relatively poor activation of the leaving group in comparison with Family I and Family II PPases. Family II-PPases have H98 as a proton donor at the bridging oxygen, where charge accumulates in the transition state [4], while Family I PPases coordinate every lone pair on the leaving group, mostly through protein sidechains [9] (Fig. 2). M-PPases, in contrast, seem to capture the PP_i in a metal cage. In addition, M-PPases bind F^- almost three orders of magnitude more weakly than Family II PPases. This is consistent with the mechanism proposed by Lin and co-workers [12], where the D287/D731 (TmPPase D236/D696) aspartate pair act as general bases to activate a water molecule for nucleophilic attack. The inability to bind F^- can be expressed another way: the water molecule in M-PPases has significantly less anionic character than in Family I and Family II PPases; the two carboxylate groups are incapable of binding an anion.

We therefore suggest that the M-PPase active site is not, in the structures currently available, set up to perform hydrolysis. If a cation is pumped out upon substrate binding, the overall negative charge at the gate would increase, which could lead to downwards motion of TM 11–12 including K499, which is ion-paired to TmPPase D236, and to downwards motion of R191, also ion-paired to D236, as is observed in the various structures (Fig. 3, [19]). Such motion would increase the basicity of the aspartate pair, activate the water nucleophile and lead to hydrolysis. Our proposal is thus that pumping drives hydrolysis, not hydrolysis, pumping. This is a binding-change mechanism. The mechanism also provides a unifying view of both sodium and proton pumping in M-PPases; there

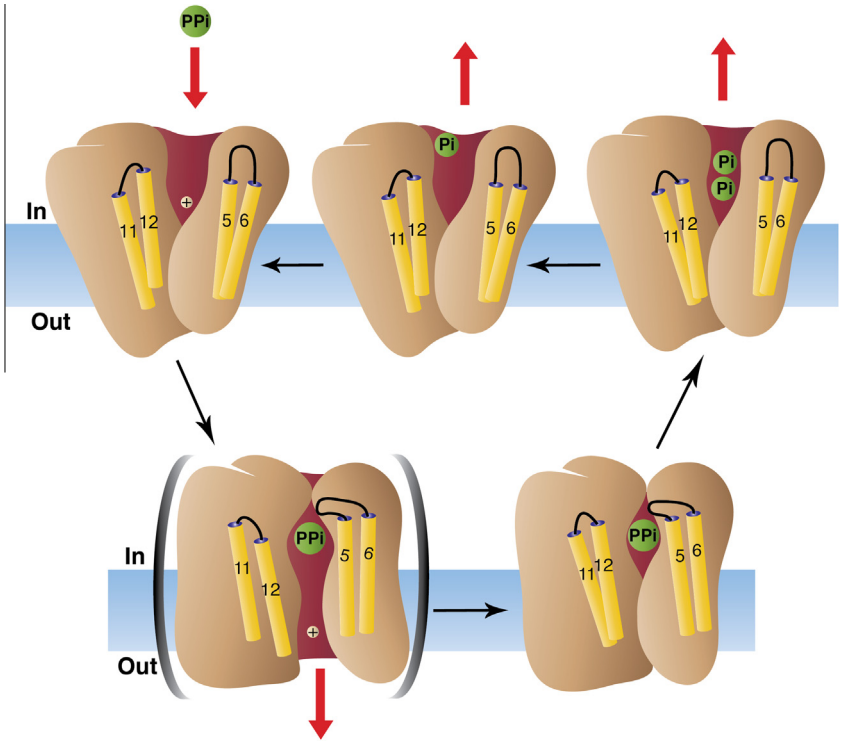

Fig. 3. Our current proposal for the catalytic cycle of M-PPases, modified from [19] with permission from the *AAAS*. Substrate binding leads to the TM 5–6 loop to close over the active site and the formation of a transient state. In this state, TM 11 and 12 move down, so that the gate and exit channel open and the Na^+ escapes to the extracellular medium. The active site stays closed until after the PP_i hydrolysis, by which time the gate and exit channel have reclosed.

would be no change in mechanism during the evolution of proton pumps from sodium pumps: a proton at the gate would be pumped during binding, with the proton from hydrolysis being released to solvent.

Whatever the atomic mechanisms of pumping and ion selectivity are, understanding them has become the final frontier in Pyrophosphatase research – and we and other laboratories are busily exploring that final frontier.

Acknowledgments

This work was supported by the European Union Seventh Framework Program EDICT (A.G.), the Sigrid Juselius Foundation (A.G.), the Academy of Finland (A.G. and T.K.), and the National Graduate School of Informational and Structural Biology (J.K.). We thank Esko Oksanen for helpful discussions.

References

[1] Lahti, R. (1983) Microbial inorganic pyrophosphatases. Microbiol. Rev. 47, 169–178.
[2] Lee, H.S., Cho, Y., Kim, Y.J., Lho, T.O., Cha, S.S., Lee, J.H. and Kang, S.G. (2009) A novel inorganic pyrophosphatase in *Thermococcus onnurineus* NA1. FEMS Microbiol. Lett. 300, 68–74.
[3] Kunitz, M. (1952) Crystalline inorganic pyrophosphatase isolated from Baker's yeast. J. Gen. Physiol. 35, 423–450.
[4] Fabrichniy, I.P., Lehtiö, L., Tammenkoski, M., Zyryanov, A.B., Oksanen, E.J., Baykov, A.A., Lahti, R. and Goldman, A. (2007) A trimetal site and ground-state substrate distortion mark the active site of family II inorganic pyrophosphatase. J. Biol. Chem. 282, 1422–1431.
[5] Baykov, A.A., Bakuleva, N.P. and Rea, P.A. (1993) Steady-state kinetics of substrate hydrolysis by vacuolar H^+-pyrophosphatase – a simple three-state model. Eur. J. Biochem. 217, 755–762.
[6] Baykov, A.A., Sergina, N.V., Evtushenko, O.A. and Dubnova, E.B. (1996) Kinetic characterization of the hydrolytic activity of the H^+-pyrophosphatase of *Rhodospirillum rubrum* in the membrane-bound and isolated states. Eur. J. Biochem. 236, 121–127.
[7] Baykov, A.A. and Shestakov, A.S. (1992) Two pathways of pyrophosphate hydrolysis and synthesis by yeast inorganic pyrophosphatase. Eur. J. Biochem. 206, 463–470.
[8] Baykov, A.A., Kasho, V.N., Bakuleva, N.P. and Rea, P.A. (1994) Oxygen exchange reactions catalyzed by vacuolar H^+-translocating pyrophosphatase. FEBS Lett. 350, 323–327.
[9] Heikinheimo, P., Lehtonen, J., Baykov, A.A., Lahti, R., Cooperman, B.S. and Goldman, A. (1996) The structural basis for pyrophosphatase catalysis. Structure 4, 1491–1508.
[10] Ahn, S., Milner, A.J., Futterer, K., Konopka, M., Ilias, M., Young, T.W. and White, S.A. (2001) The "open" and "closed" structures of the type-C inorganic pyrophosphatases from *Bacillus subtilis* and *Streptococcus gordonii*. J. Mol. Biol. 313, 797–811.
[11] Merckel, M.C., Fabrichniy, I.P., Salminen, A., Kalkkinen, N., Baykov, A.A., Lahti, R. and Goldman, A. (2001) Crystal structure of *Streptococcus mutans* pyrophosphatase: a new fold for an old mechanism. Structure 9, 289–297.
[12] Lin, S.M., Tsai, J.Y., Hsiao, C.D., Huang, Y.T., Chiu, C.L., Liu, M.H., Tung, J.Y., Liu, T.H., Pan, R.L. and Sun, Y.J. (2012) Crystal structure of membrane-embedded H^+-translocating pyrophosphatase. Nature 484, 399–403.
[13] Salminen, T., Käpylä, J., Heikinheimo, P., Goldman, A., Heinonen, J., Baykov, A.A., Cooperman, B.S. and Lahti, R. (1995) Structure and function analysis of *Escherichia coli* inorganic pyrophosphatase: is an hydroxide ion the key to catalysis? Biochemistry 34, 782–791.
[14] Oksanen, E., Ahonen, A.-K., Tuominen, H., Tuominen, V., Lahti, R., Goldman, A. and Heikinheimo, P. (2007) A complete structural description of the catalytic cycle of yeast pyrophosphatase. Biochemistry 46, 1228–1239.
[15] Jämsen, J., Tuominen, H., Salminen, A., Belogurov, G.A., Magretova, N.N., Baykov, A.A. and Lahti, R. (2007) A CBS domain-containing pyrophosphatase of *Moorella thermoacetica* is regulated by adenine nucleotides. Biochem. J. 408, 327–333.
[16] Maeshima, M. (2000) Vacuolar H^+-pyrophosphatase. Biochim. Biophys. Acta 1465, 37–51.
[17] Lopéz-Marqués, R.L., Péréz-Castineira, J.R., Losada, M. and Serrano, A. (2004) Differential regulation of soluble and membrane-bound inorganic pyrophosphatases in the photosynthetic bacterium *Rhodospirillum rubrum* provides insights into pyrophosphate-based stress bioenergetics. J. Bacteriol. 186, 5418–5426.
[18] Garcia-Contreras, R., Celis, H. and Romero, I. (2004) Importance of *Rhodospirillum rubrum* H^+-pyrophosphatase under low-energy conditions. J. Bacteriol. 186, 6651–6655.
[19] Kellosalo, J., Kajander, T., Kogan, K., Pokharel, K. and Goldman, A. (2012) The structure and catalytic cycle of a sodium pumping pyrophosphatase. Science 337, 473–476.
[20] Baykov, A.A., Malinen, A.M., Luoto, H.H. and Lahti, R. (in press) Pyrophosphate-fueled Na^+ and H^+ transport in prokaryotes. Microb. Mol. Biol. Rev.
[21] Samygina, V.R., Popov, A.N., Rodina, E.V., Vorobyeva, N.N., Lamzin, V.S., Polyakov, K.M., Kurilova, S.A., Nazarova, T.I. and Avaeva, S.M. (2001) The structures of *Escherichia coli* inorganic pyrophosphatase complexed with Ca^{2+}

or $CaPP_i$ at atomic resolution and their mechanistic implications. J. Mol. Biol. 314, 633–645.
[22] Halonen, P., Baykov, A.A., Goldman, A., Lahti, R. and Cooperman, B.S. (2002) Single turnover kinetics of *Saccharomyces cerevisiae* inorganic pyrophosphatase. Biochemistry 41, 12025–12031.
[23] Pohjanjoki, P., Fabrichniy, I.P., Kasho, V.N., Cooperman, B.S., Goldman, A., Baykov, A.A. and Lahti, R. (2001) Probing essential water in yeast pyrophosphatase by directed mutagenesis and fluoride inhibition measurements. J. Biol. Chem. 276, 434–441.
[24] Zyryanov, A.B., Pohjanjoki, P., Kasho, V.N., Shestakov, A.S., Goldman, A., Lahti, R. and Baykov, A.A. (2001) The electrophilic and leaving group phosphates in the catalytic mechanism of yeast pyrophosphatase. J. Biol. Chem. 276, 17629–17634.
[25] Heikinheimo, P., Tuominen, V., Ahonen, A.-K., Teplyakov, A., Cooperman, B.S., Baykov, A.A., Lahti, R. and Goldman, A. (2001) Toward a quantum-mechanical description of metal assisted phosphoryl transfer in pyrophosphatase. Proc. Natl. Acad. Sci. USA 98, 3121–3126.
[26] Cooperman, B.S., Baykov, A.A. and Lahti, R. (1992) Evolutionary conservation of the active site of soluble inorganic pyrophosphatase. Trends Biol. Sci. 17, 262–266.
[27] Josse, J. and Wong, S.C.K. (1971) Inorganic pyrophosphatase of *Escherichia coli*. The Enzymes 4, 499–527.
[28] Kankare, J., Neal, G.S., Salminen, T., Glumoff, T., Cooperman, B., Lahti, R. and Goldman, A. (1994) The structure of *E. coli* soluble inorganic pyrophosphatase at 2.7 Å resolution. Protein Eng. 7, 823–830.
[29] Baykov, A.A., Alexandrov, A.P. and Smirnova, I.N. (1992) A two-step mechanism of fluoride inhibition of rat liver inorganic pyrophosphatase. Arch. Biochem. Biophys. 294, 238–243.
[30] Young, T.W., Kuhn, N.J., Wadeson, A., Ward, S., Burges, D. and Cooke, G.D. (1998) *Bacillus subtilis* ORF yybQ encodes a manganese-dependent inorganic pyrophosphatase with distinctive properties: the first of a new class of soluble pyrophosphatase? Microbiology 144, 2563–2571.
[31] Shintani, T., Uchiumi, T., Yonezawa, T., Salminen, A., Baykov, A.A., Lahti, R. and Hachimori, A. (1998) Cloning and expression of a unique inorganic pyrophosphatase from *Bacillus subtilis*: evidence for a new family of enzymes. FEBS Lett. 439, 263–266.
[32] Aravind, L. and Koonin, E.V. (1998) A novel family of predicted phosphoesterases includes *Drosophila* prune protein and bacterial RecJ exonuclease. Trends Biochem. Sci. 23, 17–19.
[33] Parfenyev, A.N., Salminen, A., Halonen, P., Hachimori, A., Baykov, A.A. and Lahti, R. (2001) Quaternary structure and metal ion requirement of family II pyrophosphatases from *Bacillus subtilis*, *Streptococcus gordonii*, and *Streptococcus mutans*. J. Biol. Chem. 276, 24511–24518.
[34] Fabrichniy, I.P., Lehtiö, L., Salminen, A., Zyryanov, A.B., Baykov, A.A., Lahti, R. and Goldman, A. (2004) Structural studies of metal ions in family II pyrophosphatases: the requirement for a Janus ion. Biochemistry 43, 14403–14411.
[35] Luoto, H.H., Baykov, A.A., Lahti, R. and Malinen, A.M. (2013) Membrane-integral pyrophosphatase subfamily capable of translocating both Na^+ and H^+. Proc. Natl. Acad. Sci. USA 110, 1255–1260.
[36] Huang, Y.T., Liu, T.H., Chen, Y.W., Lee, C.H., Chen, H.H., Huang, T.W., Hsu, S.H., Lin, S.M., Pan, Y.J. and Lee, C.H. (2010) Distance variations between active sites of H^+-pyrophosphatase determined by fluorescence resonance energy transfer. J. Biol. Chem. 285, 23655–23664.
[37] Kim, E.J., Zhen, R.-G. and Rea, P.A. (1995) Site-directed mutagenesis of vacuolar H^+-pyrophosphatase. J. Biol. Chem., 2630–2635.
[38] Hsiao, Y.Y., Pan, Y.J., Hsu, S.H., Huang, Y.T., Liu, T.H., Lee, C.H., Lee, C.H., Liu, P.F., Chang, W.C., Wang, Y.K., Chien, L.F. and Pan, R.L. (2007) Functional roles of arginine residues in mung bean vacuolar H^+-pyrophosphatase. Biochim. Biophys. Acta 1767, 965–973.
[39] Hsiao, Y.Y., Van, R.C., Hung, S.H., Lin, H.H. and Pan, R.L. (2004) Roles of histidine residues in plant vacuolar H^+-pyrophosphatase. Biochim. Biophys. Acta 1608, 190–199.
[40] Yang, S.J., Jiang, S.S., Kuo, S.Y., Hung, S.H., Tam, M.F. and Pan, R.L. (1999) Localization of a carboxylic residue possibly involved in the inhibition of vacuolar H^+-pyrophosphatase by N,N′-dicyclohexylcarbodi-imide. Biochem. J. 342 (Pt 3), 641–666.
[41] Yang, S.J., Jiang, S.S., Van, R.C., Hsiao, Y.Y. and Pan, R.L. (2000) A lysine residue involved in the inhibition of vacuolar H^+-pyrophosphatase by fluorescein 5′-isothiocyanate. Biochim. Biophys. Acta 1460, 375–383.
[42] Lee, C.H., Pan, Y.J., Huang, Y.T., Liu, T.H., Hsu, S.H., Lee, C.H., Chen, Y.W., Lin, S.M., Huang, L.K. and Pan, R.L. (2011) Identification of essential lysines involved in substrate binding of vacuolar H^+-pyrophosphatase. J. Biol. Chem. 286, 11970.
[43] Gaxiola, R.A., Palmgren, M.G. and Schumacher, K. (2007) Plant proton pumps. FEBS Lett. 581, 2204–2214.
[44] McIntosh, M.T. and Vaidya, A.B. (2002) Vacuolar type H^+ pumping pyrophosphatases of parasitic protozoa. Int. J. Parasitol. 32, 1–14.
[45] Ferjani, A., Segami, S., Horiguchi, G., Muto, Y., Maeshima, M. and Tsukaya, H. (2011) Keep an eye on PPi: the vacuolar-type H^+-pyrophosphatase regulates postgerminative development in Arabidopsis. Plant Cell 23, 2895–2908.
[46] Belogurov, G.A. and Lahti, R. (2002) A lysine substitute for K^+. A460K mutation eliminates K^+ dependence in H^+-pyrophosphatase of *Carboxydothermus hydrogenoformans*. J. Biol. Chem. 277, 49651–49654.
[47] Malinen, A.M., Belogurov, G.A., Baykov, A.A. and Lahti, R. (2007) Na^+-pyrophosphatase: a novel primary sodium pump. Biochemistry 46, 8872–8878.
[48] Belogurov, G.A., Malinen, A.M., Turkina, M.V., Jalonen, U., Rytkönen, K., Baykov, A.A. and Lahti, R. (2005) Membrane-bound pyrophosphatase of *Thermotoga maritima* requires sodium for activity. Biochemistry 44, 2088–2096.
[49] Mimura, H., Nakanishi, Y., Hirono, M. and Maeshima, M. (2004) Membrane topology of the H^+-pyrophosphatase of *Streptomyces coelicolor* determined by cysteine-scanning mutagenesis. J. Biol. Chem. 279, 35106–35112.
[50] Nakanishi, Y., Saijo, T., Wada, Y. and Maeshima, M. (2001) Mutagenic analysis of functional residues in putative substrate-binding site and acidic domains of vacuolar H^+-pyrophosphatase. J. Biol. Chem. 276, 7654–7660.
[51] Takasu, A., Nakanishi, Y., Yamauchi, T. and Maeshima, M. (1997) Analysis of the substrate binding site and carboxyl terminal region of vacuolar H^+-pyrophosphatase of mung bean with peptide antibodies. J. Biochem. 122, 883–889.
[52] Nakanishi, Y., Yabe, I. and Maeshima, M. (2003) Patch clamp analysis of a H^+ pump heterologously expressed in giant yeast vacuoles. J. Biochem. (Tokyo) 134, 615–623.
[53] Malinen, A.M., Baykov, A.A. and Lahti, R. (2008) Mutual effects of cationic ligands and substrate on activity of the Na^+-transporting pyrophosphatase of *Methanosarcina mazei*. Biochemistry 47, 13447–13454.
[54] Luoto, H.H., Belogurov, G.A., Baykov, A.A., Lahti, R. and Malinen, A.M. (2011) Na^+-translocating membrane pyrophosphatases are widespread in the microbial world and evolutionarily precede H^+-translocating pyrophosphatases. J. Biol. Chem. 286, 21633–21642.
[55] Lipmann, F. (1965) Projecting backwards from the present stage of evolution of biosyntheses. The rigins of prebiological systems in: The Origins of Prebiological Systems and Their Molecular Matrices (Fox, S.W., Ed.), pp. 259–280, Academic Press, New York.
[56] Baltscheffsky, M., Schultz, A. and Baltscheffsky, H. (1999) H^+-proton-pumping inorganic pyrophosphatase: a tightly membrane-bound family. FEBS Lett. 452, 121–127.
[57] Mulkidjanian, A.Y., Dibrov, P. and Galperin, M.Y. (2008) The past and present of sodium energetics: may the sodium-motive force be with you. Biochim. Biophys. Acta 1777, 985–992.
[58] Mulkidjanian, A.Y., Galperin, M.Y., Makarova, K.S., Wolf, Y.I. and Koonin, E.V. (2008) Evolutionary primacy of sodium energetics. Biol. Direct 3, 13.
[59] Au, K.M., Barabote, R.D., Hu, K.Y. and Saier, M.H.J. (2006) Evolutionary apperance of H^+-translocating pyrophosphatase. Microbiology 152, 1243–1247.
[60] Mitchell, P. (1974) A chemiosmotic molecular mechanism for proton-translocating adenosine triphosphatases. FEBS Lett. 43, 189–194.
[61] Lanyi, J.K. (2006) Proton transfers in the bacteriorhodopsin photocycle. Biochim. Biophys. Acta 1757, 1012–1018.
[62] Smirnova, I.N., Kudryavtseva, N.A., Komissarenko, S.V., Tarusova, N.B. and Baykov, A.A. (1988) Diphosphonates are potent inhibitors of mammalian inorganic pyrophosphatase. Arch. Biochem. Biophys. 267, 280–284.
[63] Baykov, A.A., Dubnova, E.B., Bakuleva, N.P., Evtushenko, O.A., Zhen, R.-G. and Rea, P.A. (1993) Differential sensitivity of membrane-associated pyrophosphatases to inhibition by diphosphonates and fluoride delineates two classes of enzyme. FEBS Lett. 327, 199–202.
[64] Zyryanov, A.B., Lahti, R. and Baykov, A.A. (2005) Inhibition of family II pyrophosphatases by analogs of pyrophosphate and phosphate. Biochemistry (Mosc.) 70, 908–912.
[65] Baykov, A.A., Fabrichniy, I.P., Pohjanjoki, P., Zyryanov, A.B. and Lahti, R. (2000) Fluoride effects along the reactions pathways of pyrophosphatase: evidence for a second enzyme center pyrophosphate intermediate. Biochemistry 39, 11939–11947.
[66] Kurilova, S.A., Bogdanova, A.V., Nazarova, T.I. and Avaeva, S. (1984) Changes in the *Escherichia coli* inorganic pyrophosphatase activity on interaction with magnesium, zinc, calcium and fluoride ions. Bioorg. Khim. 10, 1153–1160.
[67] Avaeva, S.M. (2000) Active site interactions in oligomeric structures of inorganic pyrophosphatases. Biochemistry (Mosc.) 65, 361–372.
[68] Zyryanov, A.B., Vener, A.V., Salminen, A., Goldman, A., Lahti, R. and Baykov, A.A. (2004) Rates of elementary catalytic steps for different metal forms of the family II pyrophosphatase from *Streptococcus gordonii*. Biochemistry 43, 1065–1074.
[69] Zhen, R.G., Baykov, A.A., Bakuleva, N.P. and Rea, P.A. (1994) Aminomethylenediphosphonate: a potent type-specific inhibitor of both plant and phototrophic bacterial H^+-pyrophosphatases. Plant Physiol. 104, 153–159.
[70] Hsu, S.H., Hsiao, Y.Y., Liu, P.F., Lin, S.M., Luo, Y.Y. and Pan, R.L. (2009) Purification, characterization, and spectral analyses of histidine-tagged vacuolar H^+-pyrophosphatase expressed in yeast. Bot. Stud. 50, 291–301.
[71] Sarafian, V. and Poole, R.J. (1989) Purification of an H^+-translocating inorganic pyrophosphatase from vacuole membranes of red beet. Plant Physiol. 91, 34–38.